# EXHIBIT 37

# Appendix B: Dr. Shu-Chun Su's review of Dr. Longo's PLM methods for the identification of chrysotile

**Talc Misidentified as Chrysotile**
*- A Review of*
***MAS 71134 & M71376 Talcum Powder Analysis of Gold Bond Medicated Powder***
2022-01-30

Shu-Chun Su, Ph.D.
Technical Expert of Bulk and Airborne Asbestos Programs
National Voluntary Laboratory Accreditation Program
National Institute of Standards and Technology

Dr. Mickey E. Gunter, Emeritus University Distinguished Professor at University of Idaho, asked me to review an analytical report entitled "*MAS 71134 & M71376 Talcum Powder Analysis of Gold Bond Medicated Powder*" (MAS, 2021), which used the asbestos mineral identification method developed by this author (Su, 2003) for mineral identification.

**The Misinterpretation of the Refractive Range of Chrysotile**

The report states "*In 2003, Dr. Shu-Chun Su published a document entitled "Rapidly and Accurately Determining Refractive Induces of Asbestos Fibers by Using Dispersion Staining Method. On page 7, Table 4A & 4B shows the full range of refractive induces of chrysotile in 1.550 RI liquid at various room temperatures. At a room temperature of 21°C to 23°C (70 °F to 73 °F), Dr. Su gives the refractive index ranges for chrysotile as high as 1.580 and as low as 1.540 in the parallel direction, and for the perpendicular direction, the Su table reports a refractive index range as high as 1.579 and as low 1.541*."

MAS used Table 5 to justify that MAS's RI measurements were within Dr. Su's ranges.

Table 5
Comparison of Chrysotile Measured Refractive Indexes Between MAS, Dr. McCrone and Dr. Su

| | Refractive Index Range Parallel | Refractive Index Range Perpendicular |
|---|---|---|
| MAS | ISO 1.568 to 1.561<br>CSM 1.568 to 1.564 | ISO 1.558 to 1.550<br>CSM 1.556 to 1.550 |
| Dr. McCrone | 1.570 to 1.548 | 1.553 to 1.534 |
| Dr. Su | 1.580 to 1.540 | 1.579 to 1.541 |

MAS misinterpreted my conversion tables for chrysotile in Cargille 1.550 (Series E) R.I. liquid. Those tables do not define the ranges of chrysotile's refractive indices. Instead, they are used to convert RI matches between the liquid and solid at matching wavelengths other than 589 nm, back to the reported values that are given at 589 nm. (Details for this are given in Su, 1993, 1998, 2003A and 2003B)

**The Identity of Crystal P in M71376-001ISO-001 is Not Chrysotile**

On p.131, MAS identified a tiny platy single crystal, which I have labeled P, in the Sample M71376-001ISO-001 to be chrysotile because of an R.I. of 1.567 parallel to its major axis and 1.552 perpendicular to its major axis (the same crystal on p.132), based on the observed CSDS (central stop dispersion staining) colors. The rule of thumb of applying CSDS technique to refractive index determination is the use of the maximum possible intensity of microscope illumination and the adequate adjustment of both field and aperture diaphragms to properly bring out the CSDS color (Fig. 1). MAS's original micrograph clearly indicated how a subdued microscope illumination could severely distort the observation of the right CSDS color. Table 1 compares the observation and conclusion made by MAS and this author.

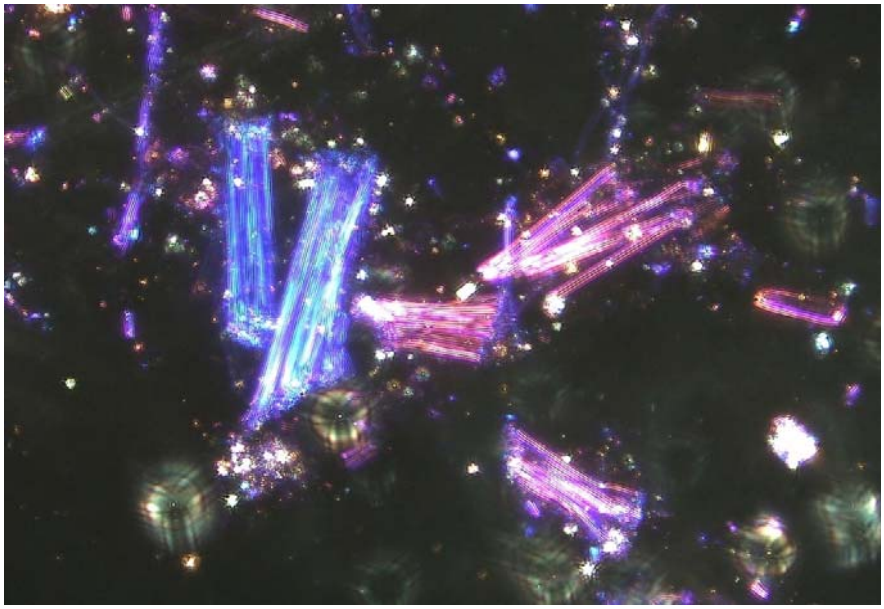

Fig. 1. The CSDS colors of NIST SRM (Standard Reference Material) 1866 chrysotile ($\alpha = 1.549$; $\gamma = 1.556$) in 1.550 high dispersion RI liquid at 23℃. E-W polarizer.

Table 1. The crystal P in sample M71376-001ISO-001 measured at 21℃ (MAS, 2021).

| Property | | MAS (A in Figs. 2 & 3) | Author (B in Figs. 2 & 3) |
|---|---|---|---|
| Microscope illumination | | Subdued | Adjusted to normal |
| Morphology | | No description | Platy |
| Parallel to major axis or γ (p.131) | CSDS color | Golden yellow | Pale yellow |
| | Matching wavelength | 460 nm | <400 nm |
| | Refractive index | 1.567 | 1.589 |
| Perpendicular to major axis or α (p.132) | CSDS color | Purple | Pale blue-green |
| | Matching wavelength | 589 nm | 700 nm |
| | Refractive index | 1.552 | 1.543 |
| CSDS color to matching wavelength conversion | | McCrone (Table 2) | McCrone (Table 2) |
| Matching wavelength to RI conversion | | Chrysotile in Cargille 1.550 (Table 3) | Talc in Cargille 1.550 (Table 4) |
| Identification | | Chrysotile | Talc |

Table 2. The Conversion of dispersion staining color to the corresponding matching wavelength $\lambda_0$ (McCrone, 1987)

| **Matching Wavelength $\lambda_0$, nm** | **Particle Edge DS Colors[1]** | | **Becke Line Colors[2]** | |
|---|---|---|---|---|
| | **Annular Stop[3]** | **Central Stop[4]** | **Particle** | **Liquid** |
| **<340** | Black violet | white | white | X |
| **<400** | dark violet | pale yellow | pale yellow | X |
| **430** | violet | yellow | pale yellow | X |
| **455** | blue | golden yellow | yellow | violet |
| **485** | blue-green | orange | orange | violet |
| **520** | green | red purple | orange-red | violet-blue |
| **560** | yellow-green | purple | red-orange | blue-violet |
| **595** | yellow | deep blue | red | blue |
| **625** | orange | blue-green | faint red | blue |
| **660** | red-brown | light blue-green | X | blue-green |
| **700** | dark red-brown | pale blue-green | X | pale blue-green |
| **1500** | black-brown | very pale blue-green | X | very pale blue-green |

Table 3. The conversion of the matching wavelength $\lambda_0$ to the corresponding RI value for chrysotile in Cargille 1.550 (Series E) RI liquid (Su, 2003B)

Table 4A. **Chrysotile α** (In Cargille Series **E**: **1.550**)

| $\lambda_0$ | 19°C | 21°C | 23°C | 25°C | 27°C | 29°C | 31°C |
|---|---|---|---|---|---|---|---|
| 400 | 1.583 | 1.582 | 1.581 | 1.580 | 1.579 | 1.578 | 1.577 |
| 420 | 1.577 | 1.576 | 1.575 | 1.574 | 1.573 | 1.572 | 1.571 |
| 440 | 1.573 | 1.572 | 1.571 | 1.570 | 1.569 | 1.568 | 1.567 |
| 460 | 1.569 | 1.568 | 1.567 | 1.566 | 1.565 | 1.564 | 1.563 |
| 480 | 1.565 | 1.564 | 1.563 | 1.562 | 1.561 | 1.560 | 1.559 |
| 500 | 1.562 | 1.561 | 1.560 | 1.559 | 1.558 | 1.557 | 1.556 |
| 520 | 1.560 | 1.559 | 1.558 | 1.557 | 1.556 | 1.555 | 1.554 |
| 540 | 1.558 | 1.557 | 1.556 | 1.555 | 1.554 | 1.553 | 1.552 |
| 560 | 1.556 | 1.555 | 1.554 | 1.553 | 1.552 | 1.551 | 1.550 |
| 580 | 1.554 | 1.553 | 1.552 | 1.551 | 1.550 | 1.549 | 1.548 |
| 589 | 1.553 | 1.552 | 1.551 | 1.550 | 1.549 | 1.548 | 1.547 |
| 600 | 1.552 | 1.551 | 1.550 | 1.549 | 1.548 | 1.547 | 1.546 |
| 620 | 1.551 | 1.550 | 1.549 | 1.548 | 1.547 | 1.546 | 1.545 |
| 640 | 1.549 | 1.548 | 1.547 | 1.546 | 1.545 | 1.544 | 1.543 |
| 660 | 1.548 | 1.547 | 1.546 | 1.545 | 1.544 | 1.543 | 1.542 |
| 680 | 1.547 | 1.546 | 1.545 | 1.544 | 1.543 | 1.542 | 1.541 |
| 700 | 1.546 | 1.545 | 1.544 | 1.543 | 1.542 | 1.541 | 1.540 |
| 750 | 1.544 | 1.543 | 1.542 | 1.541 | 1.540 | 1.539 | 1.538 |
| 800 | 1.542 | 1.541 | 1.540 | 1.539 | 1.538 | 1.537 | 1.536 |

Table 4B. **Chrysotile γ** (In Cargille Series **E**: **1.550**)

| $\lambda_0$ | 19°C | 21°C | 23°C | 25°C | 27°C | 29°C | 31°C |
|---|---|---|---|---|---|---|---|
| 400 | 1.581 | 1.580 | 1.579 | 1.578 | 1.577 | 1.576 | 1.575 |
| 420 | 1.575 | 1.574 | 1.573 | 1.572 | 1.571 | 1.570 | 1.569 |
| 440 | 1.571 | 1.570 | 1.569 | 1.568 | 1.567 | 1.566 | 1.565 |
| 460 | 1.567 | 1.566 | 1.565 | 1.565 | 1.564 | 1.563 | 1.562 |
| 480 | 1.564 | 1.563 | 1.562 | 1.561 | 1.560 | 1.559 | 1.558 |
| 500 | 1.562 | 1.561 | 1.560 | 1.559 | 1.558 | 1.557 | 1.556 |
| 520 | 1.559 | 1.558 | 1.557 | 1.556 | 1.555 | 1.554 | 1.553 |
| 540 | 1.557 | 1.556 | 1.555 | 1.554 | 1.553 | 1.552 | 1.551 |
| 560 | 1.555 | 1.554 | 1.553 | 1.552 | 1.551 | 1.550 | 1.549 |
| 580 | 1.554 | 1.553 | 1.552 | 1.551 | 1.550 | 1.549 | 1.548 |
| 589 | 1.553 | 1.552 | 1.551 | 1.550 | 1.549 | 1.548 | 1.547 |
| 600 | 1.552 | 1.551 | 1.550 | 1.549 | 1.548 | 1.547 | 1.546 |
| 620 | 1.551 | 1.550 | 1.549 | 1.548 | 1.547 | 1.546 | 1.545 |
| 640 | 1.550 | 1.549 | 1.548 | 1.547 | 1.546 | 1.545 | 1.544 |
| 660 | 1.548 | 1.547 | 1.546 | 1.546 | 1.545 | 1.544 | 1.543 |
| 680 | 1.547 | 1.546 | 1.545 | 1.544 | 1.544 | 1.543 | 1.542 |
| 700 | 1.546 | 1.546 | 1.545 | 1.544 | 1.543 | 1.542 | 1.541 |
| 750 | 1.544 | 1.543 | 1.542 | 1.541 | 1.540 | 1.540 | 1.539 |
| 800 | 1.543 | 1.542 | 1.541 | 1.540 | 1.539 | 1.538 | 1.537 |

Dispersion coefficients: Cargille 1.550 (Series E) Liquid 0.0267; Chrysotile α 0.0107, γ 0.0119.

Table 4. The conversion of the matching wavelength $\lambda_m$ (equivalent to $\lambda_0$ in Table 2 and 3) to the corresponding refractive index for talc in Cargille 1.550 (Series E) RI liquid (Su, 2022. Constructed specifically for this review)

**Talc in Cargille 1.550 (E)**

| $\lambda_m$ | α | | | | | | γ | | | | | |
|---|---|---|---|---|---|---|---|---|---|---|---|---|
| (nm) | 19°C | 21°C | 23°C | 25°C | 27°C | 29°C | 19°C | 21°C | 23°C | 25°C | 27°C | 29°C |
| **300** | 1.662 | 1.661 | 1.660 | 1.659 | 1.658 | 1.658 | 1.662 | 1.661 | 1.660 | 1.659 | 1.658 | 1.657 |
| **320** | 1.638 | 1.637 | 1.636 | 1.635 | 1.634 | 1.633 | 1.637 | 1.636 | 1.635 | 1.634 | 1.633 | 1.633 |
| **340** | 1.620 | 1.619 | 1.618 | 1.617 | 1.616 | 1.616 | 1.620 | 1.619 | 1.618 | 1.617 | 1.616 | 1.615 |
| **360** | 1.607 | 1.606 | 1.605 | 1.604 | 1.603 | 1.602 | 1.607 | 1.606 | 1.605 | 1.604 | 1.603 | 1.602 |
| **380** | 1.597 | 1.596 | 1.595 | 1.594 | 1.593 | 1.592 | 1.596 | 1.596 | 1.595 | 1.594 | 1.593 | 1.592 |
| **400** | 1.588 | 1.588 | 1.587 | 1.586 | 1.585 | 1.584 | 1.588 | 1.587 | 1.586 | 1.586 | 1.585 | 1.584 |
| **420** | 1.582 | 1.581 | 1.580 | 1.579 | 1.578 | 1.577 | 1.582 | 1.581 | 1.580 | 1.579 | 1.578 | 1.577 |
| **440** | 1.576 | 1.575 | 1.574 | 1.573 | 1.573 | 1.572 | 1.576 | 1.575 | 1.574 | 1.573 | 1.572 | 1.572 |
| **460** | 1.571 | 1.571 | 1.570 | 1.569 | 1.568 | 1.567 | 1.571 | 1.570 | 1.570 | 1.569 | 1.568 | 1.567 |
| **480** | 1.567 | 1.567 | 1.566 | 1.565 | 1.564 | 1.563 | 1.567 | 1.566 | 1.566 | 1.565 | 1.564 | 1.563 |
| **500** | 1.564 | 1.563 | 1.562 | 1.561 | 1.560 | 1.559 | 1.564 | 1.563 | 1.562 | 1.561 | 1.560 | 1.559 |
| **520** | 1.561 | 1.560 | 1.559 | 1.558 | 1.557 | 1.556 | 1.561 | 1.560 | 1.559 | 1.558 | 1.557 | 1.556 |
| **540** | 1.558 | 1.557 | 1.556 | 1.555 | 1.555 | 1.554 | 1.558 | 1.557 | 1.556 | 1.555 | 1.555 | 1.554 |
| **560** | 1.556 | 1.555 | 1.554 | 1.553 | 1.552 | 1.551 | 1.556 | 1.555 | 1.554 | 1.553 | 1.552 | 1.551 |
| **580** | 1.554 | 1.553 | 1.552 | 1.551 | 1.550 | 1.549 | 1.554 | 1.553 | 1.552 | 1.551 | 1.550 | 1.549 |
| **600** | 1.552 | 1.551 | 1.550 | 1.549 | 1.548 | 1.547 | 1.552 | 1.551 | 1.550 | 1.549 | 1.548 | 1.547 |
| **620** | 1.550 | 1.549 | 1.548 | 1.547 | 1.546 | 1.545 | 1.550 | 1.549 | 1.548 | 1.547 | 1.546 | 1.545 |
| **640** | 1.548 | 1.547 | 1.547 | 1.546 | 1.545 | 1.544 | 1.548 | 1.547 | 1.547 | 1.546 | 1.545 | 1.544 |
| **660** | 1.547 | 1.546 | 1.545 | 1.544 | 1.543 | 1.542 | 1.547 | 1.546 | 1.545 | 1.544 | 1.543 | 1.542 |
| **680** | 1.546 | 1.545 | 1.544 | 1.543 | 1.542 | 1.541 | 1.546 | 1.545 | 1.544 | 1.543 | 1.542 | 1.541 |
| **700** | 1.544 | 1.543 | 1.542 | 1.542 | 1.541 | 1.540 | 1.544 | 1.543 | 1.543 | 1.542 | 1.541 | 1.540 |
| **720** | 1.543 | 1.542 | 1.541 | 1.540 | 1.540 | 1.539 | 1.543 | 1.542 | 1.541 | 1.541 | 1.540 | 1.539 |
| **740** | 1.542 | 1.541 | 1.540 | 1.539 | 1.539 | 1.538 | 1.542 | 1.541 | 1.540 | 1.539 | 1.539 | 1.538 |
| **760** | 1.541 | 1.540 | 1.539 | 1.538 | 1.538 | 1.537 | 1.541 | 1.540 | 1.539 | 1.538 | 1.538 | 1.537 |
| **780** | 1.540 | 1.539 | 1.538 | 1.538 | 1.537 | 1.536 | 1.540 | 1.539 | 1.538 | 1.538 | 1.537 | 1.536 |
| **800** | 1.539 | 1.538 | 1.538 | 1.537 | 1.536 | 1.535 | 1.539 | 1.539 | 1.538 | 1.537 | 1.536 | 1.535 |
| **850** | 1.538 | 1.537 | 1.536 | 1.535 | 1.534 | 1.533 | 1.538 | 1.537 | 1.536 | 1.535 | 1.534 | 1.533 |
| **900** | 1.536 | 1.535 | 1.534 | 1.533 | 1.532 | 1.531 | 1.536 | 1.535 | 1.534 | 1.533 | 1.532 | 1.531 |
| **950** | 1.534 | 1.534 | 1.533 | 1.532 | 1.531 | 1.530 | 1.535 | 1.534 | 1.533 | 1.532 | 1.531 | 1.530 |
| **1000** | 1.533 | 1.532 | 1.531 | 1.531 | 1.530 | 1.529 | 1.533 | 1.532 | 1.532 | 1.531 | 1.530 | 1.529 |

Dispersion coefficients: Cargille 1.550 (Series E) Liquid 0.0267; Talc α 0.0075, γ 0.0076.

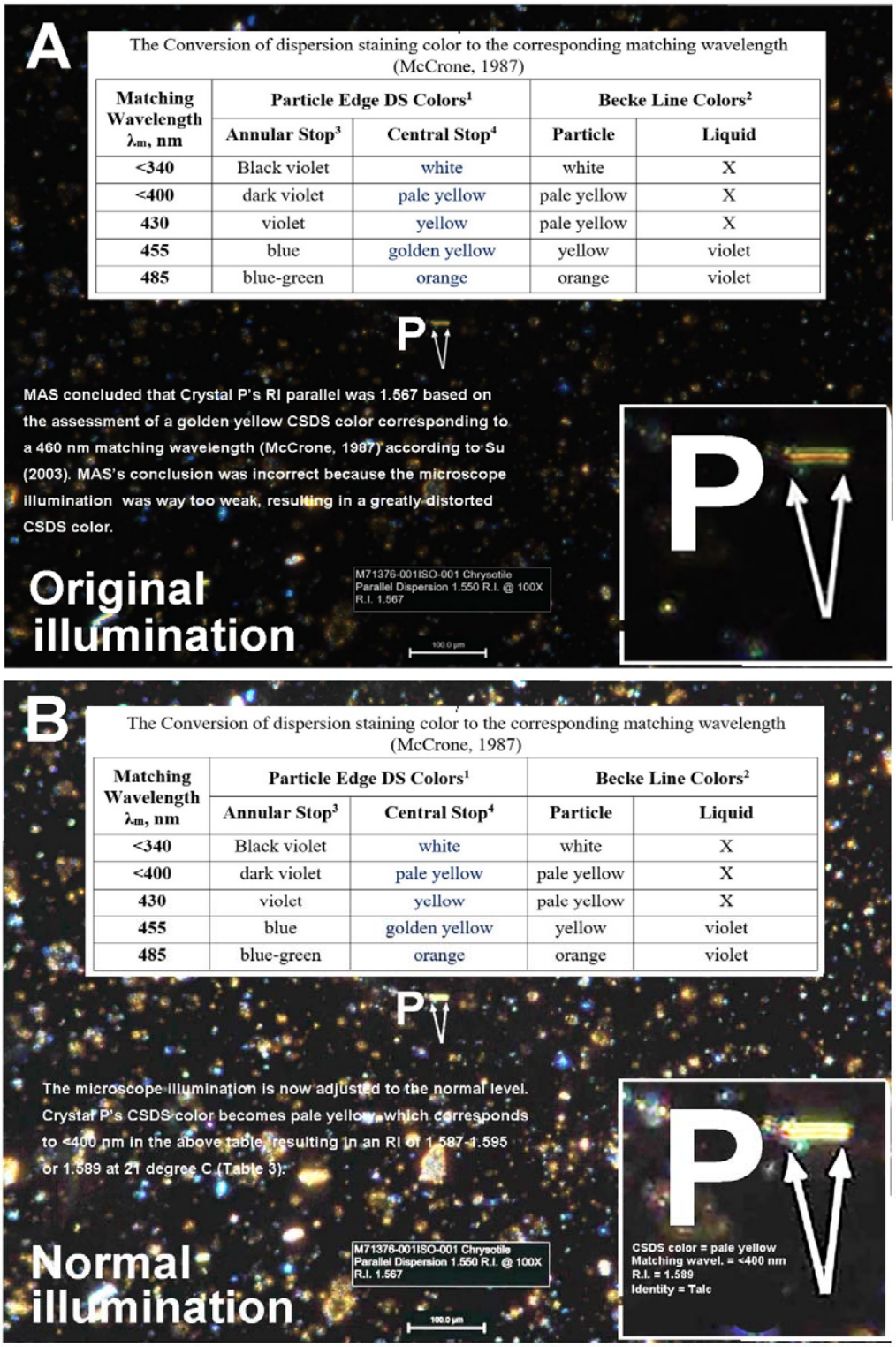


Fig. 2. Crystal P's γ of M71376-001-ISO-001 (p.131, MAS, 2021)

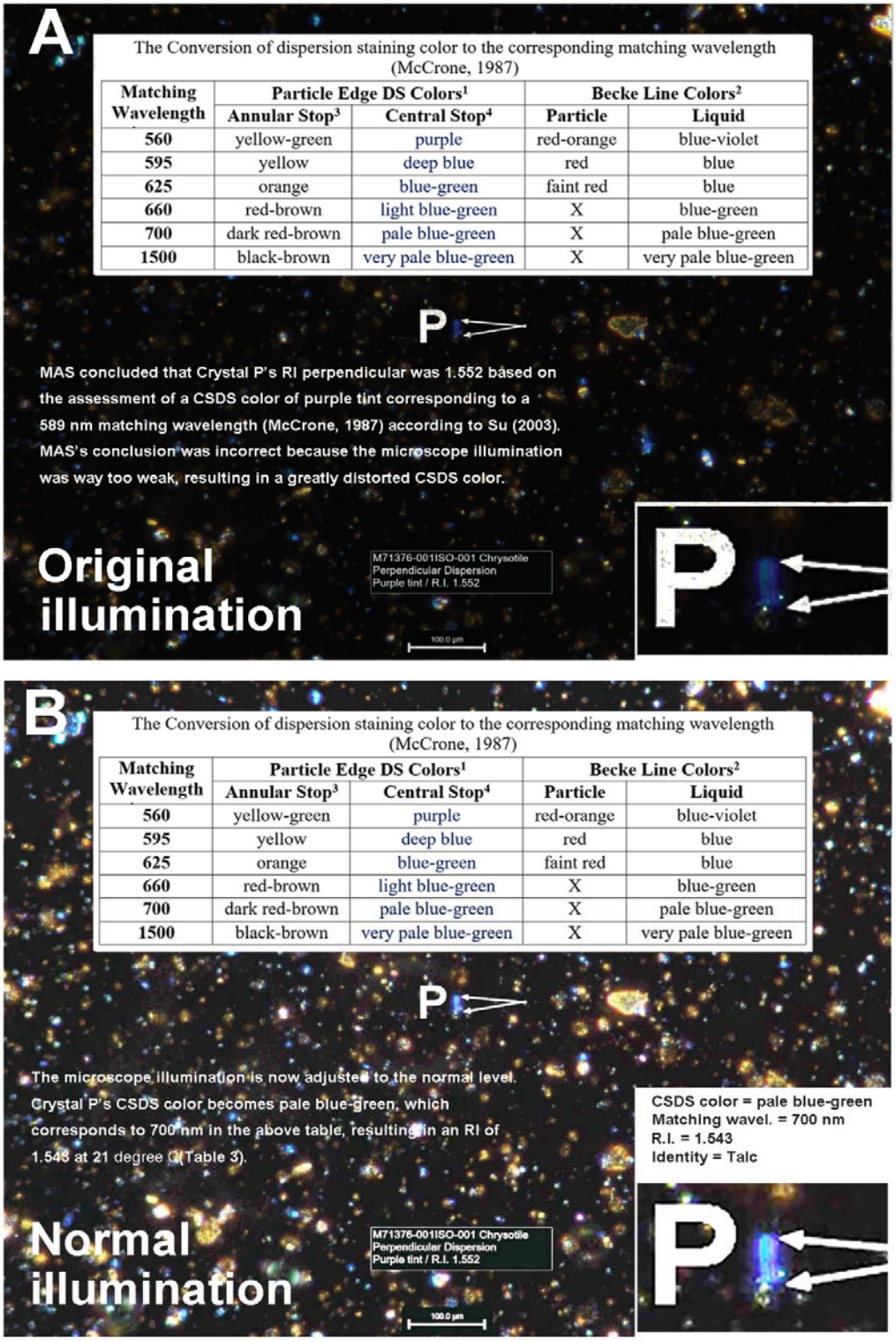


Fig. 3. Crystal P's α of M71376-001-ISO-001 (p.132, MAS, 2021)

**Evidences of the Misidentification of Chrysotile**

The Asbestos Hazard Emergency Response Act (AHERA), United States Code 15 (U.S.C., 1982) mandates the use of U.S. Environmental Protection Agency (EPA) protocol (U.S. EPA, 1982) for the analysis of asbestos content in bulk materials, which is followed by MAS in the analysis of Gold Bond Medicated Powder. The analysis uses stereomicroscopy and polarized light microscopy (PLM) to identify and quantify the asbestos minerals in bulk materials, requiring the measurement of morphology and six optical properties: color, pleochroism, refractive index (RI), birefringence, extinction, and sign of elongation. Among those properties, morphology and RI are the most important and diagnostic properties. It is exactly in these two crucial diagnostic properties the crystal P in sample M71376-001ISO-001 does not conform to the characteristics of chrysotile.

1. Morphology

Fig. 1 shows a typical chrysotile under CSDS observation by polarized light microscopy. Chrysotile never occurs as single crystal in nature. It always occurs as fiber bundles (usually a few tenths of a μm to a few μm) consisting of fine fibrils (usually a few hundredths of a μm) as shown in Fig. 1. The crystal P is a typical plate in Fig. 2 without fine fibril texture does not conform to chrysotile morphology at all.

2. Refractive index

The 1.567 assignment of the RI along the crystal plate's major axis is incorrect. It does not conform to chrysotile's γ, whose CSDS color is normally magenta and never in the yellow range. The yellowish CSDS color in Fig. 2 only proves that the crystal has an RI significantly greater than 1.550. The exact amount above 1.550 can only be established by a second measurement in 1.570 or 1.580, an immersion liquid whose RI is greater than the crystal. It is a common knowledge that, among the range of CSDS color, yellow is the least reliable one because unlike purple, magenta, etc. it is very subjective to distinguish among golden yellow, yellow, pale yellow (Table 2). In other words, it is extremely difficult to accurately find out the corresponding matching wavelength, resulting in very inaccurate RI. Another unavoidable complication is that the yellow CSDS color is very sensitive to the microscope illumination or the intensity of the microscope light source. Other factors significantly affecting the yellow CSDS color are the opening of the field and aperture diaphragms and the distance between the sample slide and the substage condenser.

In this case, the rule of thumb is to ***bring the yellow CSDS color to purple or magenta or blue range*** by using an immersion liquid with a greater RI, such as 1.560 or 1.570 for crystal P at a ***normal intensity of illumination*** such as B in Fig. 2.

By increasing the brightness of the micrographs on p. 131 to the normal level of Fig. 1, a clearly-defined CSDS color, which is a clearly pale yellow, was resulted for the same crystal as shown in Fig. 2. According to Table 4, the corresponding matching wavelength $\lambda_m$ is <400 nm, resulting in an RI of 1.587-1.596 or 1.589.

Using the same approach, crystal P in the micrograph of p. 132 and Fig. 3 shows a clearly-defined CSDS color of pale blue-green, resulting in an RI of 1.543.

**The Above Analysis is Equally Applicable to the Other Six Samples in the Report, Namely M71376-001-ISO-002, 003, 004, 005, 006, and 007**

The subdued illumination problem is common to the other six samples in the report. By increasing their illumination to the normal level, M71376-001-ISO-002, 003, 004, and 005 shows optical properties characteristic of talc with 005's higher than normal α. None of the large

ribbon particles in M71376-001-ISO-006 and 007 is chrysotile. They are actually cellulose fiber contaminants.

A. γ original illumination

B. γ normal illumination

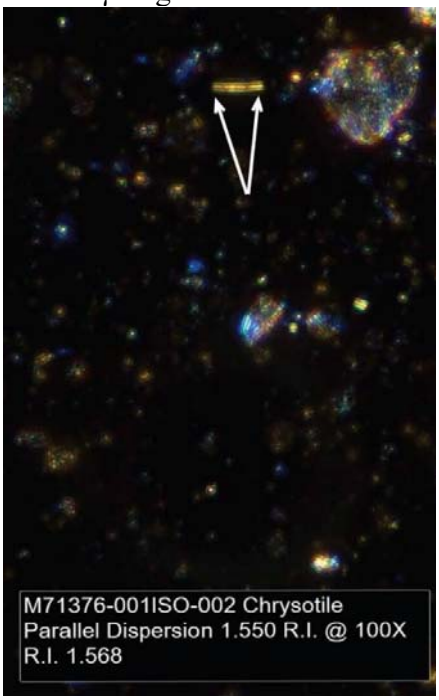


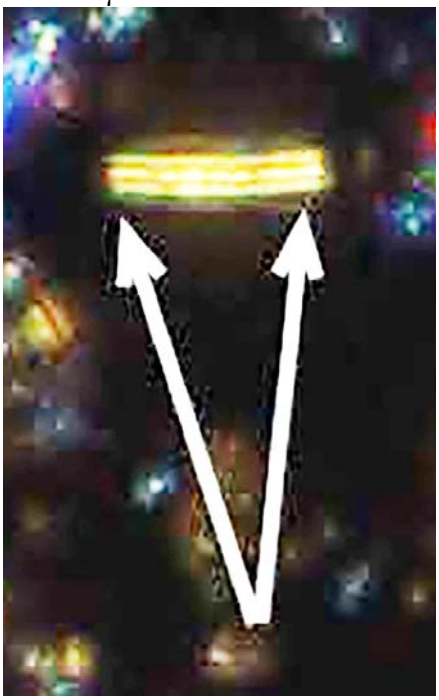

C. α original illumination

D. α normal illumination

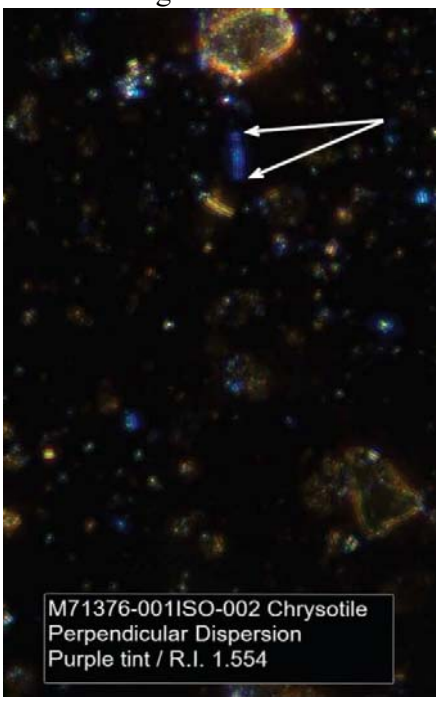


Fig. 4. M71376-001-ISO-002

A. γ original illumination

B. γ normal illumination

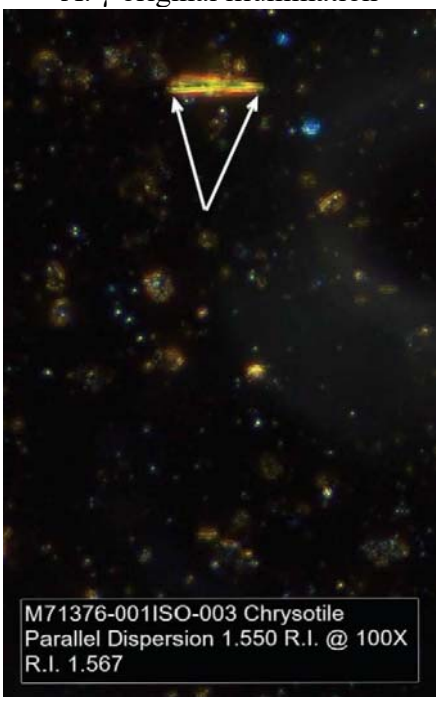


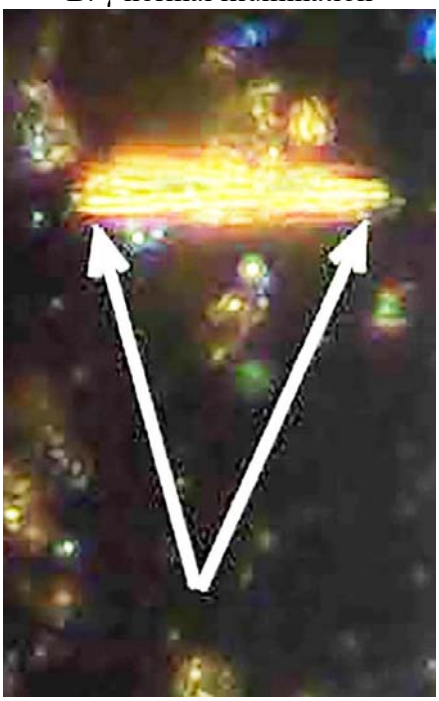

C. α original illumination

D. α normal illumination

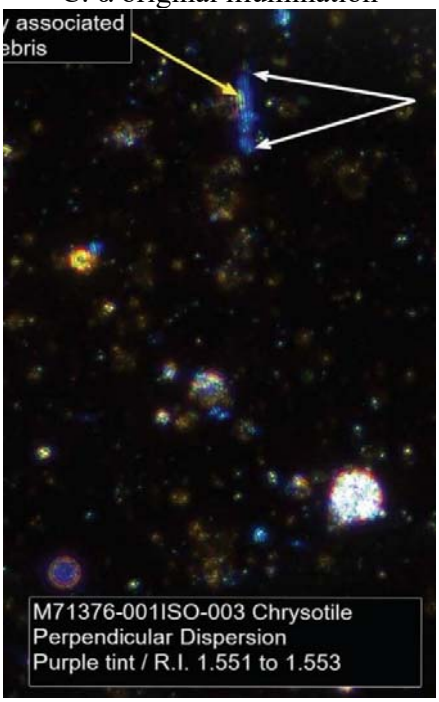


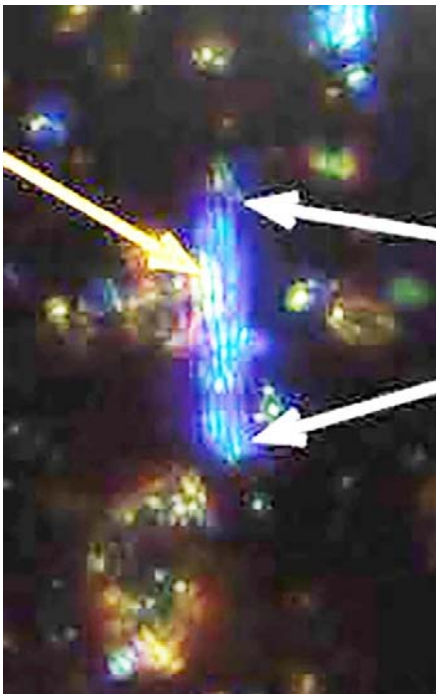

Fig. 5. M71376-001-ISO-003

A. γ original illumination

B. γ normal illumination

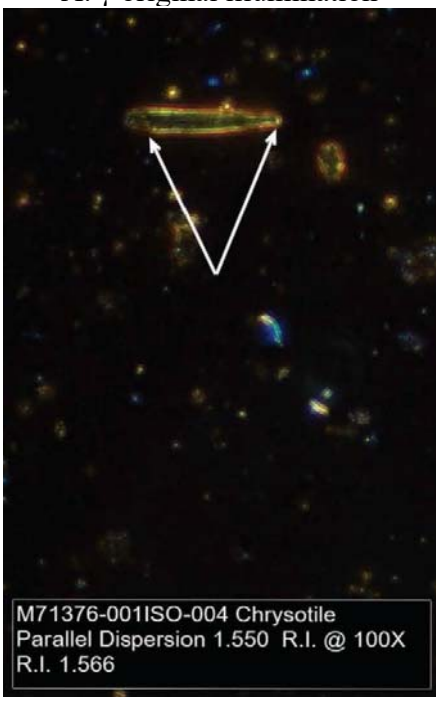


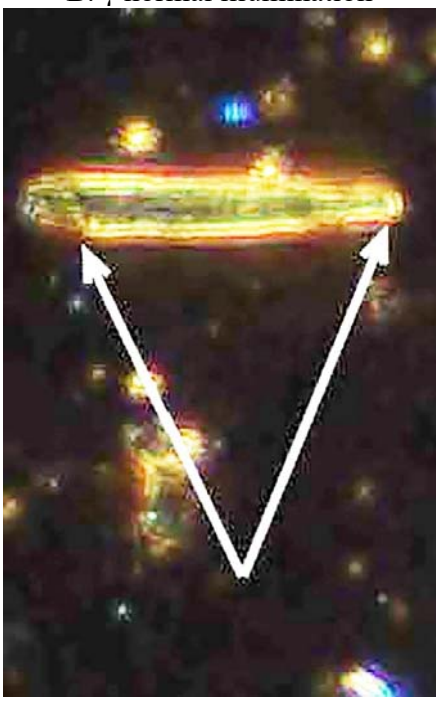

C. α original illumination

D. α normal illumination

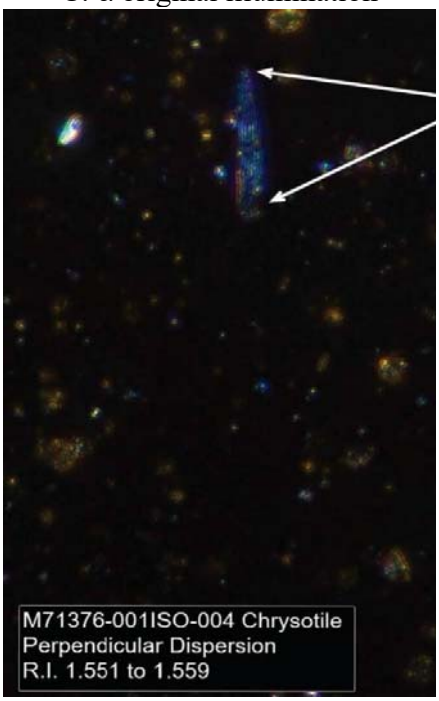


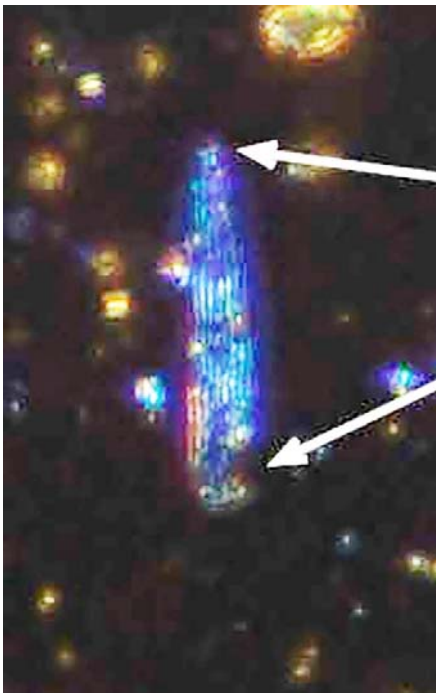

Fig. 6. M71376-001-ISO-004

A. γ original illumination

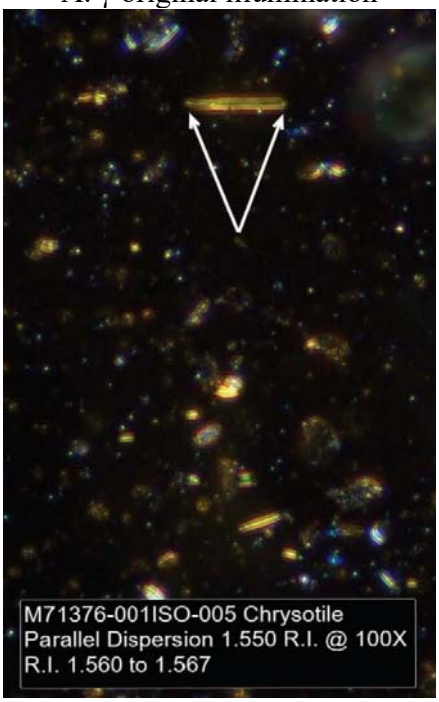


B. γ normal illumination

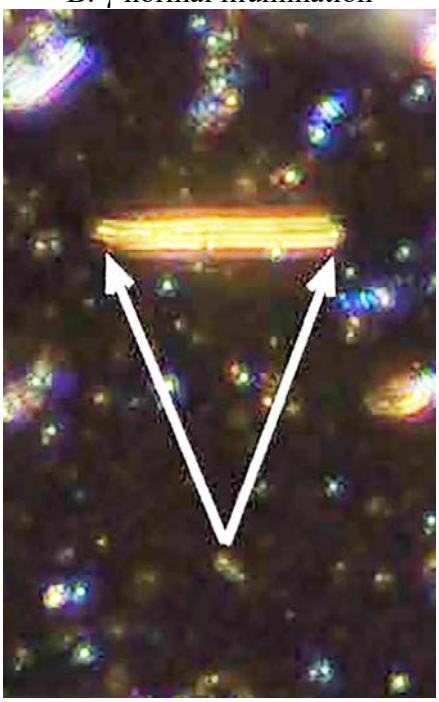

C. α original illumination

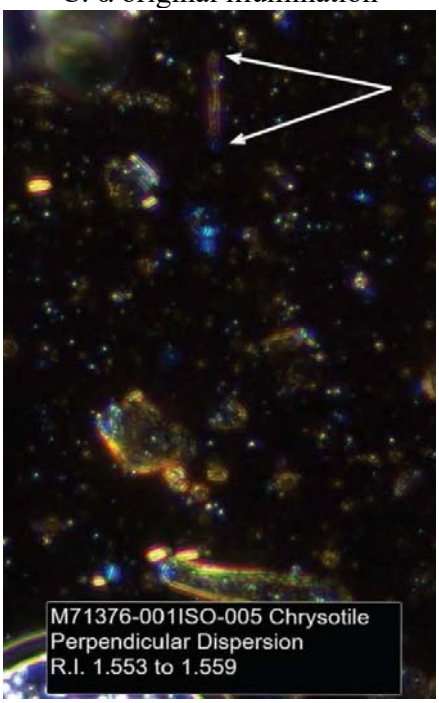


D. α normal illumination

Fig. 7. M71376-001-ISO-005

A. γ original illumination

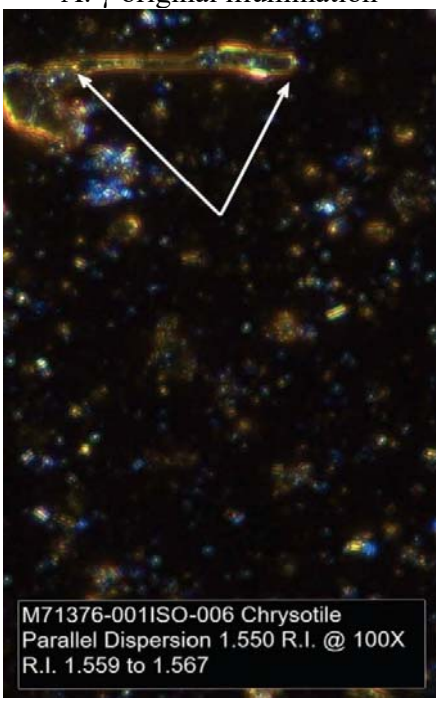


B. γ normal illumination

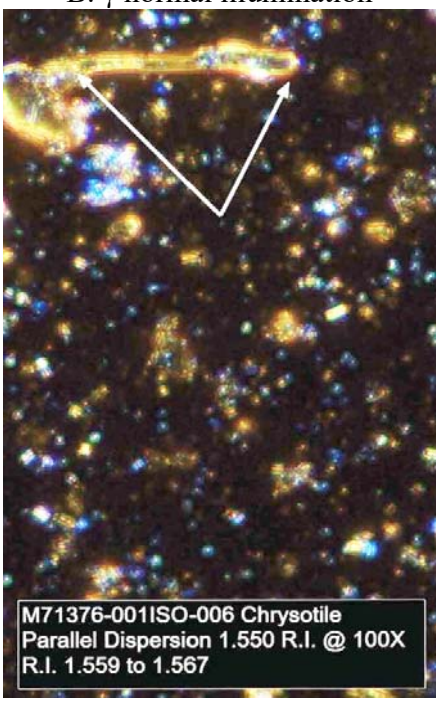


C. α original illumination

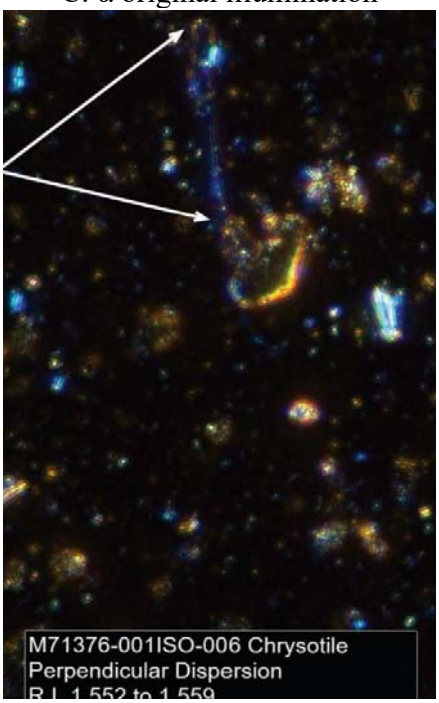


D. α normal illumination

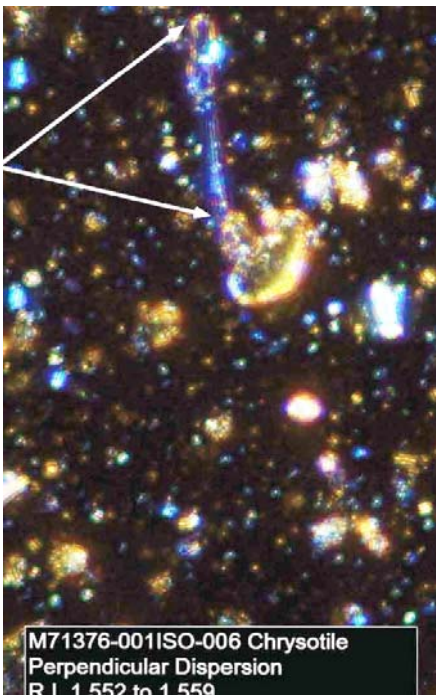


Fig. 8. M71376-001-ISO-006

A. γ original illumination

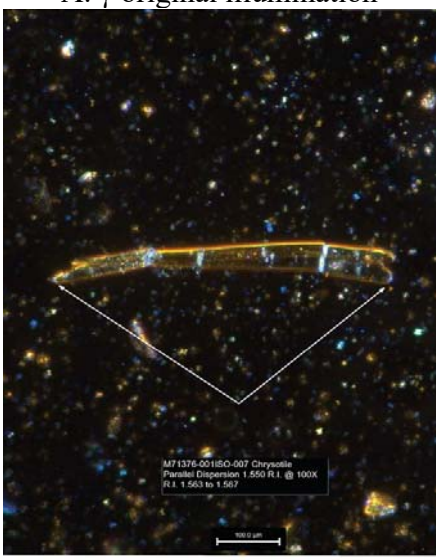


B. γ normal illumination

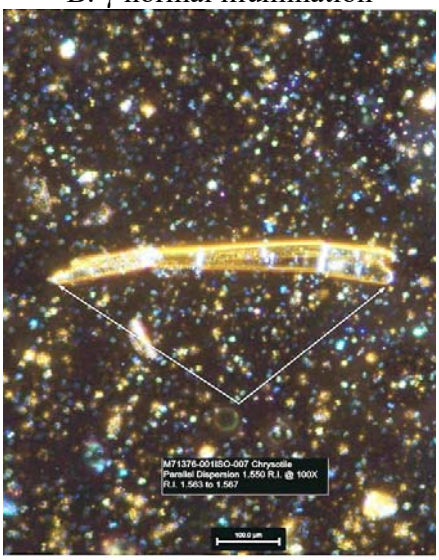


C. α original illumination

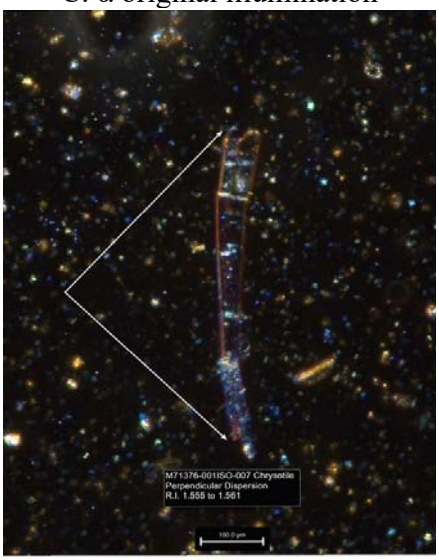


D. α normal illumination

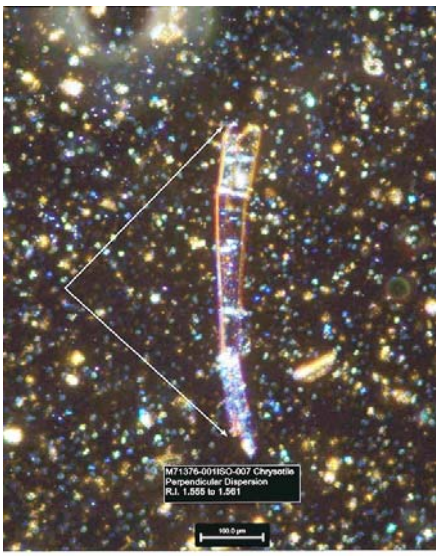


Fig. 9. M71376-001-ISO-007

**Conclusion**

Based on the evidences of morphology and refractive indices, crystal P in Sample M71376-001-ISO-001 as well as all the arrowed crystals in Samples M71376-001-ISO-002, 003, 004, and 005, are talc instead of chrysotile, whereas M71376-001-ISO-006 and 007 are cellulose fibers.

**References**

MAS (2021) MAS 71134 & M71376 Talcum Powder Analysis of Gold Bond Medicated Powder.

McCrone, W. C. (1987) Asbestos Identification. McCrone Research Institute. Chicago.

Su, S. C. (1993) Determination of Refractive Index of Solids by Dispersion Staining Method - An Analytical Approach. Rieder, C. L., Ed., Proceedings of 51st Annual Meeting of the Microscopy Society of America, 456-457.

Su, S. C. (1998) Dispersion Staining: Principles, Analytical Relationships and Practical Applications to the Determination of Refractive Index. The Microscope, 46, 123-146.

Su, S. C. (2003A) A Rapid and Accurate Procedure for the Determination of Refractive Indices of Asbestos Minerals. American Mineralogist, 88, 1979-1982.

Su, S. C. (2003B) Rapidly and Accurately Determining Refractive Indices of Asbestos Fibers by Using Dispersion Staining Method - A Standard Operation Procedure for Bulk Asbestos Analysis by Polarized Light Microscopy. Asbestos Analysis Consulting Ltd.

U.S.C. (1986) Asbestos Hazard Emergency Response Act. Title 15 - Commerce and Trade Chapter 53 - Toxic Substances Control, Subchapter II.

U.S. EPA (1982) 40 CFR Appendix E to Subpart E of Part 763, Interim Method of the Determination of Asbestos in Bulk Insulation Samples.